Variable Waist-Diameter Mach-Zehnder Tapered-Fiber Interferometer as Humidity and Temperature Sensor

M. R. K. Soltanian, A. S. Sharbirin, M. M. Ariannejad, I. S. Amiri, R. M. De La Rue, G. Brambilla, B. M. A. Rahman, K. T. V. Grattan and H. Ahmad

***Abstract*— In-line single-mode tapered-fiber Mach-Zehnder interferometers (MZI-SMTF) with average waist diameters (d_{avg}) of 4.05 and 2.89 µm have been fabricated - and both the temperature and the humidity sensitivity of the surrounding media have been measured and compared. The humidity and temperature were measured over the ranges from 0% to 90% and 28 ºC to 40 ºC, respectively. The stability of the system at 50%RH and 90%RH were investigated while the temperature of the chamber was maintained at about 28 ºC. The humidity and temperature sensitivity resolution values were 0.02 nm/%RH and 0.05 nm/0.1ºC for the MZI-SMTF-1 with an average waist diameter of 4.05 µm – while they were 0.01 nm/%RH and 0.025 nm/0.1ºC for the MZI-SMTF-2 with an average waist diameter of 2.89 µm.**

***Index Terms*— Fiber sensor, Inline MZI, Tapered fiber, Humidity sensor, Temperature sensor.**

I. Introduction

HUMIDITY and temperature monitoring are vital in various industrial applications, e.g. the production of chemical substances, mining activities and inbiomedical plants since it enables control of product quality and protection of workers' health. Additionally it is important in the avoidance and control of corrosion in large structures - for example aircraft and bridges [1]. Subsequently, there has been extensive analysis on relative humidity (RH) and temperature sensors in various approaches including capacitive, resistive and optical humidity and temperature sensors. The humidity and temperature sensor market has been monopolized by electronic digital sensors. Nevertheless, due to advances in the field of fiber optical sensing, niche applications can be found where fiber optical humidity and temperature sensors can strongly compete with their electronics humidity and temperature counterparts.

This work has been supported under Grants LRGS(2015) NGOD/UM/KPT, UM.C/625/1/HIR/MOHE/SCI/29, GA010-2014 (ulung) and RU007/2015. (*Corresponding author:H Ahmad*)

MRK Soltanian, AS Sharbirin, MM Ariannejhad, IS Amiri and H Ahmad are with the Photonics Research Center University of Malaya 50603 Kuala Lumpur, Federal Territory of Kuala Lumpur (e-mail: soltanian79@gmail.com; anirsyazwan92@gmail.com; cpu4202002@gmail.com; isafiz@yahoo.com; harith@um.edu.my).

RM De La Rue is with Department of Electronics and Electrical Engineering, University of Glasgow, Glasgow, G12 8LT, UK (e-mail: rmdelarue@gmail.com)

G Brambilla is with Optoelectronics Research Center, University of Southampton, Southampton, UK (e-mail: gilberto@soton.ac.uk)

B. M. A. Rahman, K. T. V. Grattan are with School of Mathematics, Computer Science and Engineering, City University London, Northampton Square, London, EC1V 0HB, UK (e-mail: b.m.a.rahman@city.ac.uk; k.t.v.grattan@city.ac.uk)

Transmit a huge amount of data taken from optical sensors over a long distance, due to large bandwidth and low attenuation of optical fiber give their market a huge priority. On top of that, the application of several approaches to interrogation enable the applications to design distributed humidity and temperature sensor [2]. In addition, the electromagnetic interference is one the main issue for the electrical humidity and temperature sensors and it prevents utilization of this kind of sensors. Moreover, the small dimensions of the optical fiber sensors make them suitable to packaging into lightweight devices or embedded in polymer materials ergonomically. Last but not least, the sensitivity of optical fiber sensors are normally higher than the conventional sensors once they operate at high resolution [3], [4]. The guided light in the fiber core and the surrounding medium (evanescent field effect for tapered fiber) collected in fiber optic humidity sensors (FOHS).

Meanwhile the ambient temperature and humidity changes the surrounding medium's refractive index. Consequently, it affects the transmission and reflection of the guided light that interacts with the surrounding medium. Optical fiber humidity sensors are currently a topic of major research interest [5-9] that mostly utilize the interaction of the evanescent field of the tapered fiber with the surrounding. An optical humidity sensor based on reversible absorption of water from the surrounding medium of tapered fiber in vicinity of spongy thin film interferometer has been reported by Muto *et. al*. [10]. The thin film refractive index changes by absorption of water and consequently transforms the lossy fiber into a light guide. A similar humidity sensor based on deposition of nanostructured film on the tapered fibers has been introduced by Corres *et. al*. [11] utilizing the ionic self-assembled monolayer (ISAM) deposition technique [12, 13].

By simultaneous use of heating and stretching, optical microfibers can be created from regular-sized ordinary optical single mode fiber (SMF) and tapered [14] to achieve a uniform waist region size that is comparable to the optical wavelength - together with a biconical lengthwise shape. The taper profile can be fine-tuned for use in different applications by controlling the pulling rate during the fabrication process [15, 16]. The typical desired characteristics for utilizing microfibers in optical sensing are large evanescent fields, flexibility, strong optical confinement, robustness and configurability. In 2005, Lou *et. al.* provided a design for a microfiber-MZI optical sensor for refractive index measurement in liquid environments by using numerical calculations. In that work, they predicted a sensitivity that was one order of magnitude better than those presented by conventional SMF-MZIs [17]. In 2002, Wo and

his group, introduced a sensor based on refractive index by using a microfiber MZI [18]. When the 2 μm waist diameter size microfiber was utilized as a sensing arm, the sensor showed a RI sensitivity of 7159 μm/RIU. A microfiber-MZI-based current sensor was reported by Jasim *et. al.*, where the results showed a slope efficiency of 60.17 pm/A^2 [19].

This paper describes the experimental demonstration of variable microfiber MZIs, with different waist diameters, that experience a shift of the dip the transmission spectrum when the environmental humidity and temperature of the external medium are altered. These effects have been verified in the 1.5 μm wavelength region that is considered to be a common and accessible wavelength region, due to availability of low cost components. The shift is relatively uniform and stable, and is appropriate for applications in sensing. Additionally, the taper uniformity and waist diameter of the tapered fiber can be accurately controlled during the tapering process. The interferometric technique is used to operate the optical sensor. Subsequently, the optical transmission spectrum of the MZI with respect to small changes in both the RH and temperature is investigated.

II. Background Theory

Light propagates within a micro- and nano-fiber (MNF) when a difference exists between the core and cladding refractive indices - and the effective index consistently decreases along the down-taper transition. Consequently, the taper modes propagate and are guided and confined by the cladding-air interface. Mode propagation in the MNF can be analyzed using Maxwell's equations [20, 21] the weakly confined propagation approximation in air - so that:

$$\left[\frac{J_\nu(U)}{UJ_\nu(U)}+\frac{K_\nu(U)}{WK_\nu(U)}\right]\left[\frac{J_\nu(U)}{UJ_\nu(U)}+\left(\frac{n_{surr}}{n_{MNF}}\right)^2\frac{K_\nu(U)}{WK_\nu(U)}\right]=\nu^2\left(\frac{1}{U^2}+\frac{1}{W^2}\right)\left(\frac{1}{U^2}+\left(\frac{n_{surr}}{n_{MNF}}\right)^2\frac{1}{W^2}\right) \quad (1)$$

where

$$U=r\sqrt{k_0^2n_{MNF}^2-\beta^2},\quad W=r\sqrt{\beta^2-k_0^2n_{surr}^2}, \quad (2)$$

and J_ν is the ν^{th}-order Bessel function of the first kind, K_ν is the ν^{th}-order modified Bessel function of the second kind, n_{MNF} and n_{surr} are the refractive indices of the MNF and the surrounding medium respectively, β is the effective propagation constant of the optical mode, r is the core radius and corresponds to the distance from the fiber axis to the core-cladding interface in solid fibers - or to the cladding-air interface in MNFs. The propagation constant for these hybrid modes can be calculated by solving equation 1. The V number can be expressed as:

$$V=\sqrt{U^2+W^2}=\frac{2\pi}{\lambda}\cdot r\cdot NA \quad (3)$$

MNFs experience single-mode operation when $V < 2.405$ and a large portion of the power will propagate as the evanescent field outside the MNF for $V << 1$ [22].

III. Experimental Setup

The Mach-Zehnder microfiber used in this experiment was fabricated from a standard SMF-28 optical fiber having a 9 μm core diameter and NA of 0.14. This optical fiber was tapered using a modified Mach-3 computer numerically-controlled (CNC) machine, which allowed for fabrication of a tapered fiber with propagation losses lower than 0.1 dB and a uniform waist diameter. This SMTF is illustrated in figure 1. A gradual reduction of the core and cladding diameters in a single-mode tapered-fiber (SMTF) will cause the evanescent fields to spread out into the cladding. These evanescent fields can reach the outer boundary for particular values of the SMTF waist diameter, since the fiber core is reduced to such an extent that its wave guiding effect is rendered negligible and light instead becomes guided by the interface between the cladding and the external medium. i.e. the whole reduced-diameter fiber forms the waveguide core. It is important to note that the circular symmetry of the original fiber is preserved, to a close approximation, throughout the SMTF, regardless of the diameter. The uniform-waist region lengths, L_1 and L_2, for all samples used in this experiment, as shown in figure1, were kept constant and equal to 20 mm - and the eventual waist diameters, d_1 and d_2, of the tapered fibers were changed in this experiment - in order to investigate the humidity sensing dependence of the Mach-Zehnder microfiber interferometer, while using different waist diameters.

Fig. 1. MZI-SMTF with uniform waist lengths L_1 and L_2, waist diameters of d_1 and d_2 and MZI-SMTF arm length of L.

Figure 2 shows the experimental set-up used to measure changes in the RH of the system, in a home-made humidity and temperature chamber. A tunable laser source (YOKOGAWA AQ2211) is synchronized with the YOKOGAWA AQ6370B optical spectrum analyzer (OSA) to provide a wide supercontinuum laser source from 1440 nm to 1640 nm.

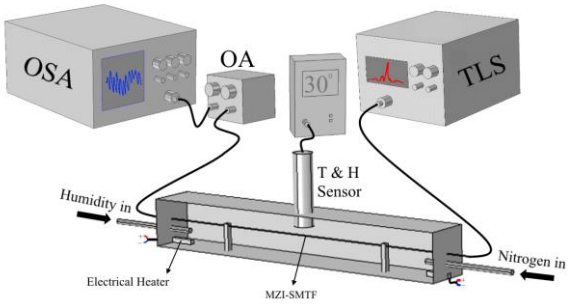

Fig. 2. Experimental set-up for measurement of changes in RH using different MZI-STFM waist-diameters.

The laser source is connected to the OSA through the MZI-SMTF and the optical attenuator (OA) respectively to measure small changes in the humidity and temperature inside the

humidity chamber. The humidity inside the chamber is controlled by balancing the amount of Nitrogen gas and humidity in the chamber. The temperature inside the chamber is controlled and tuned using the two electrical filaments located at the two corners of the chamber, as shown in figure 2. The temperature and humidity inside the chamber is measured by using a HANNA instruments HI thermos hygrometer Thermal and humidity sensor.

The free spectral range (FSR) is directly related to the length of the MZI-STMF, *L*, and it is about 0.55 nm for the both fabricated MZI-SMTF. The transmission spectrum of the MZI-STMF-1 shown in figure 3.

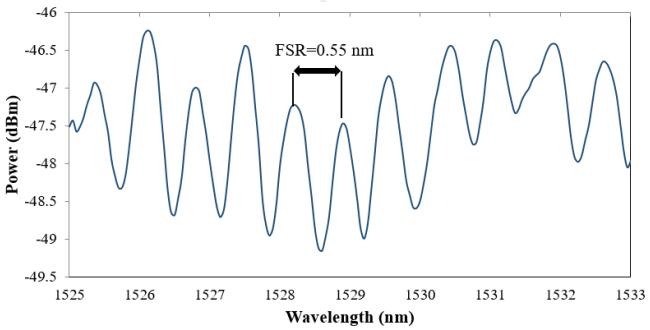

Fig. 3. Transmission spectrum of the MZI-SMTF-1.

The first tapered area served to diffract the fundamental mode, and consequently to allow both the core and the cladding modes to become excited. Phase shifting within a physical length, *L*, of the MZI-SMTF is a result of the unequal effective refractive indices of the core and cladding modes. The different phase velocity of the fundamental and cladding modes cause a phase difference along the MZI-SMTF arm, due to MZI-SMTF's length dependency and variation of wavelength of the guided light. The transmitted optical power of the interferometer will be minimized at certain wavelength and maximized at the others due to wavelength dependency of phase difference and phase velocity. The separation between consecutive peaks of a two-mode interferometer is given by $\Delta\lambda=\lambda^2/L\Delta n_e$, where λ indicates the source wavelength, *L* is the length of the MZI-STMF - and Δn_e symbolizes the effective refractive index difference between the core and cladding (external medium) modes.

IV. Results and Discussion

The transmission spectrum of the MZI-SMTF shown in figure 3 is the result of constructive and destructive interference between the cladding and core modes introduced into the MZI-SMTF, which generate an interference pattern in the MZI-SMTF. Since the two tapered regions, L1 and L2, act as a beam-splitter and combiner - and changes in the refractive index of the surrounding medium lead to changes in the output transmission spectrum. Two different waist-diameter MZI-SMTFs were fabricated: firstly to investigate the effect of the waist diameter of the fabricated MZI-SMTF on its resolution as a temperature and humidity sensor and secondly to measure the temperature and humidity changes in the surrounding environment of the MZI-SMTF. Table 1 provides information about the parameters of the two fabricated MZI-SMTFs used in this experiment.

TABLE I. Parameters for the two fabricated MZI-SMTFs

	L (mm)	L_1 (mm)	L_2 (mm)	d_1 (μm)	d_2 (μm)	d_{avg} (μm)
MZI-SMTF-1	100	20	20	3.75	4.53	4.05
MZI-SMTF-2	100	20	20	3.55	2.09	2.82

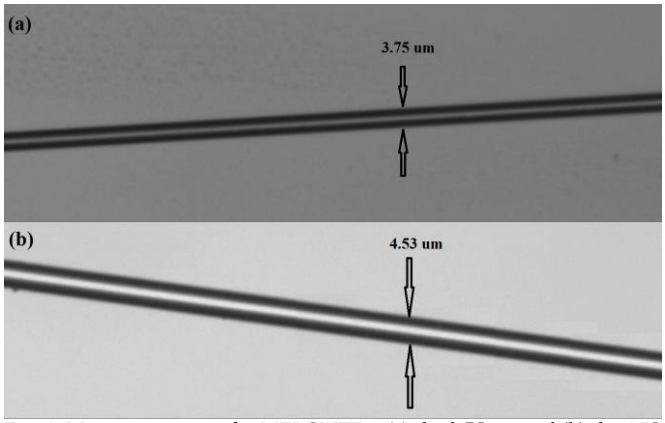

Fig. 4. Microscope image for MZI-SMTF-1 (a) $d_1 =$ 3.75 μm and (b) $d_2 =$ 4.53 μm.

Microscope images of the two tapered regions for MZI-SMTF-1 are shown in figure 4. The displacement of the transmission spectrum produced by changes in the refractive index that result from either humidity or temperature changes inside the humidity and temperature chamber surroundings of MZI-SMTF-1 are shown in figure 5. The displacement of the transmission spectrum was measured for humidity changing from 0%RH to 90%RH, with the temperature maintained constant - and temperature changing from 29 ºC to 40 ºC, with the RH kept constant.

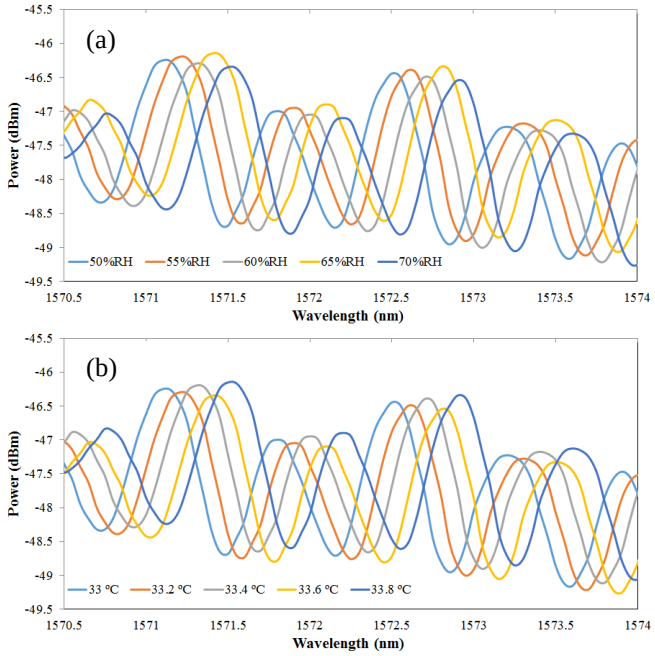

Fig. 5. (a) The displacement of the transmission spectrum for the MZI-SMTF-1corresponding to changing (a) the RH and (b) the temperature.

Figure 5(a) illustrates the displacement of the transmission spectrum produced by changing the RH for five different values - 50%RH, 55%RH, 60%RH, 65%RH and 70%

RH - while the temperature in the chamber was kept constant at 30 ºC. Figure 5(b) presents the displacement of the transmission spectrum produced by variation of the chamber temperature - for measured temperatures of 33 ºC, 33.2 ºC, 33.4 ºC, 33.6 ºC and 33.8 ºC - while the humidity of the chamber was kept constant at 50%RH.

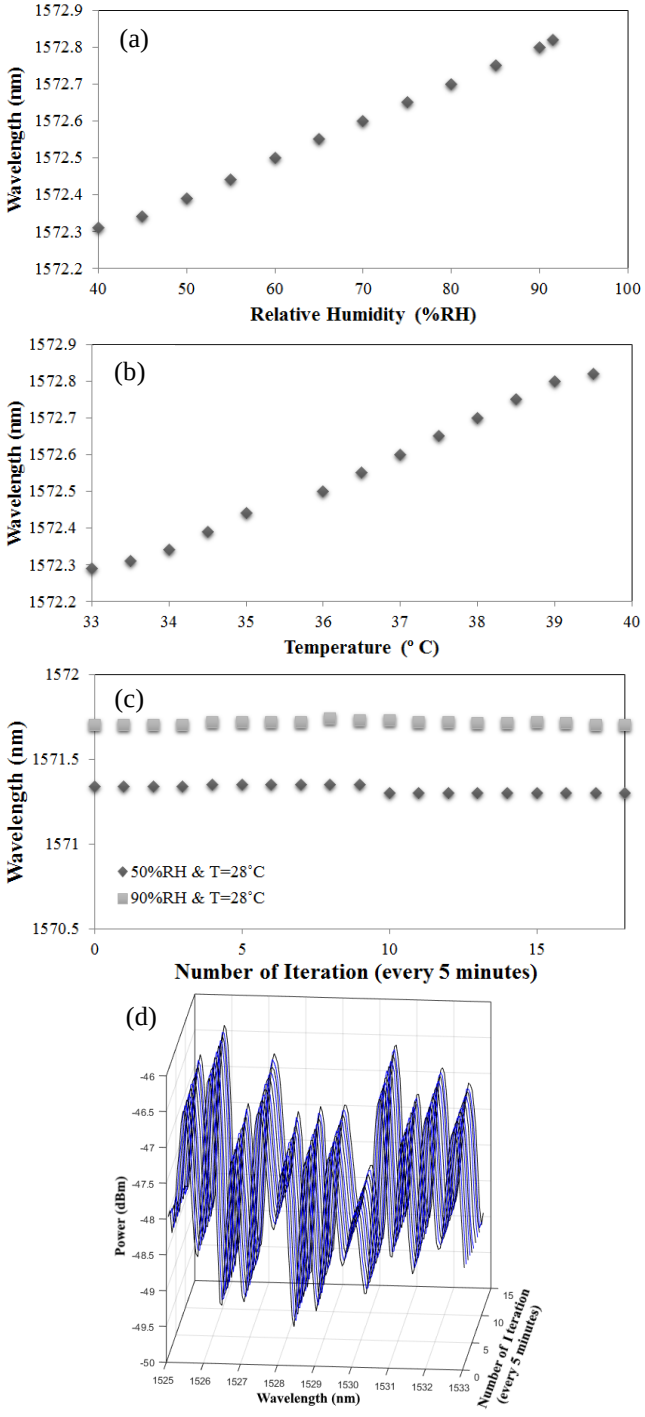

Fig. 6. Displacement of the MZI-SMTF-1 transmission spectrum for changing (a) RH and (b) temperature, inside the chamber. (c) Stability of the system at 50%RH and 90%RH, with the temperature of the chamber remaining unchanged. (d) The stability of the MZI-SMTF-1 transmission spectrum over a 90 minute period during which the humidity and temperature were maintained at 50%RH and 28 ºC, respectively.

Figure 6(a) and (b) show the displacement of the MZI-SMTF-1 transmission spectrum for changes in both RH and temperature, respectively, inside the chamber - as the refractive index of the medium surrounding the MZI-SMTF-1 changed. As can be observed, the humidity and temperature sensitivities of the MZI-SMTF-1 are 0.02 nm/%RH and 0.05 nm/0.1ºC, respectively. Figure 6(c) illustrates the stability of the system at 50%RH and 90%RH, while the temperature of the chamber remained unchanged at about 28 ºC. Figure 6(d) shows the stability of the MZI-SMTF-1 transmission spectrum over a 90 minute period - during which the humidity and temperature remained unchanged at 50%RH and 28 ºC, respectively.

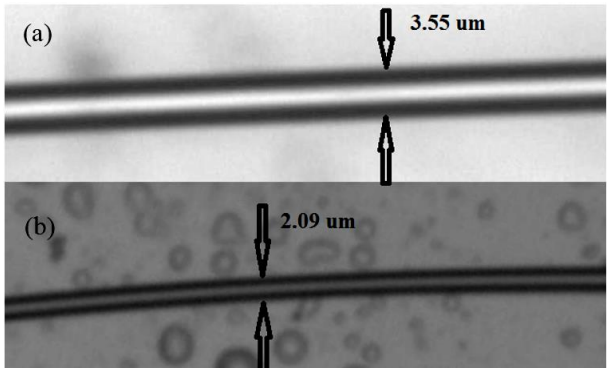

Fig. 7. Microscope image for MZI-SMTF-2 (a) $d_1 = 3.55$ µm and (b) $d_2 = 2.09$ µm.

Figure 7 shows microscope images of the two tapered regions for MZI-SMTF-2. The displacement of the transmission spectrum due to changes in the refractive index as a result of either humidity changing or temperature changing in the chamber surrounding MZI-SMTF-2 is shown in figure 8.

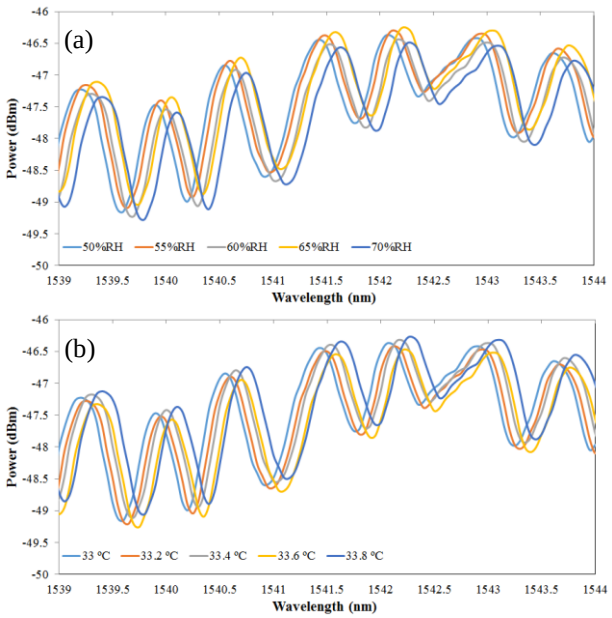

Fig. 8. The displacement of the transmission spectrum for the MZI-SMTF-2 corresponding to changing the (a) RH and (b) temperature.

The displacement of the transmission spectrum was measured for the humidity changing from 0%RH to 90%RH with the temperature remaining constant - and temperature

changing from 29 ºC to 40 ºC with the RH remaining unchanged.

Figure 8(a) illustrates the displacement of the transmission spectrum produced by changing the RH for five different RH values - 50%RH, 55%RH, 60%RH, 65%RH and 70% RH, while the temperature in the chamber was maintained at 30 ºC. Figure 8(b) presents the displacement of the transmission spectrum produced by variation of chamber temperature for the measured temperatures of 33 ºC, 33.2 ºC, 33.4 ºC, 33.6 ºC and 33.8 ºC, while the humidity of the chamber remained constant at 50%RH.

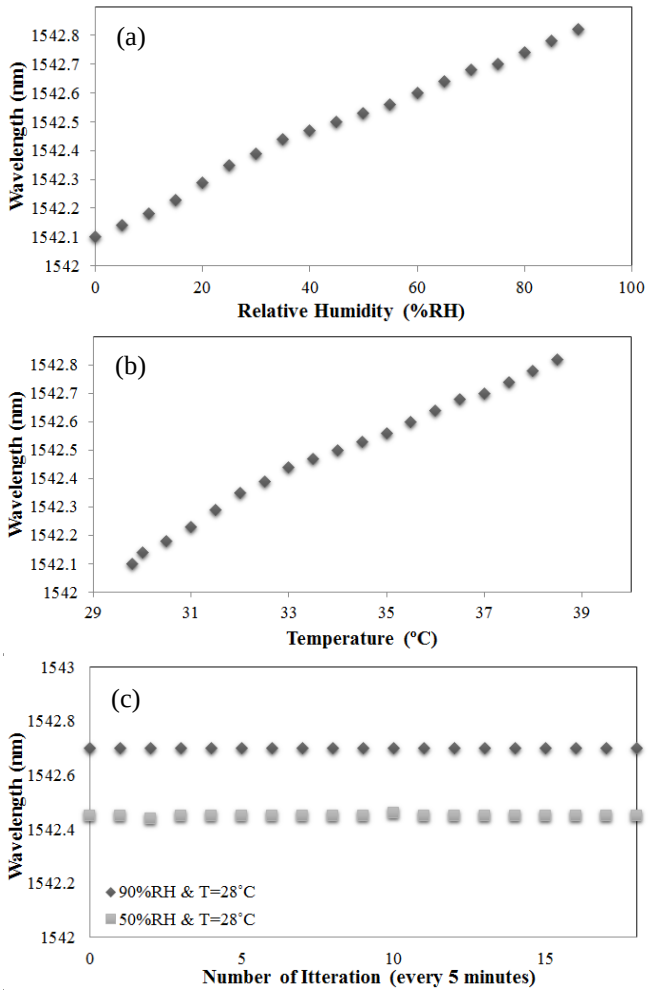

Fig. 9. Displacement of the MZI-SMTF-2 transmission spectrum for changes in: (a) RH - and (b) temperature, inside the chamber. (c) Stability of the system in 50%RH and 90%RH while the temperature of the chamber remained unchanged.

Figure 9 (a) and (b) show the displacement of the MZI-SMTF-2 transmission spectrum for changes in RH and temperature inside the chamber, respectively - as the refractive index of the medium surrounding the MZI-SMTF-2 changed. As can be seen, the humidity and temperature sensitivities of the MZI-SMTF-2 are 0.01 nm/%RH and 0.025 nm/0.1ºC respectively. Figure 9(c) illustrates the stability of the system at 50%RH and 90%RH, while the temperature of the chamber remained unchanged at about 28 ºC.

V. Conclusion

Two different waist-diameter, simple in-line, single-mode, tapered-fiber Mach-Zenhder interferometers (MZI-SMTF), with average waist diameters, (d_{avg}), of 4.05 and 2.89 µm respectively, have been fabricated. The fabricated MZI-SMTF performed based on interferometric techniques to operate the optical sensor where the transmission spectrum of the MZI-SMTF with respect to small changes in both the RH and the temperature was investigated. The performance of the sensors was investigated for probes with variable different taper waist-diameters. It was observed that the output transmission spectra shifted when the RH and temperature levels increased. The resolution achieved increases when the average waist diameter of the MZI-SMTF decreases. The humidity and temperature sensitivity values for MZI-SMTF-1 were 0.02 nm/%RH and 0.05 nm/0.1ºC, respectively - while the humidity and temperature sensitivity values for MZI-SMTF-2 were 0.01 nm/%RH and 0.025 nm/0.1ºC, respectively. These sensors are easy to fabricate, cheap - and compact. Although the MZI-SMTF's waist diameters and lengths directly affect the sensor resolution, small fluctuation on MZI-SMTF's waist diameters could be ignored. Moreover, fabricating such MZI-SMTF by utilizing accurate tapered machine will minimize the fabrication errors and cause the device reproducibility.

References

[1] A. Sun, Z. Li, T. Wei, Y. Li, and P. Cui, "Highly sensitive humidity sensor at low humidity based on the quaternized polypyrrole composite film," *Sensors and Actuators B: Chemical*, vol. 142, pp. 197-203, 2009.

[2] Q. Wu, Y. Semenova, P. Wang, and G. Farrell, "High sensitivity SMS fiber structure based refractometer–analysis and experiment," *Optics Express*, vol. 19, pp. 7937-7944, 2011.

[3] T.-S. Cho, K.-S. Choi, D.-C. Seo, I.-B. Kwon, and J.-R. Lee, "Novel fiber optic sensor probe with a pair of highly reflected connectors and a vessel of water absorption material for water leak detection," *Sensors*, vol. 12, pp. 10906-10919, 2012.

[4] J. Lou, Y. Wang, and L. Tong, "Microfiber optical sensors: A review," *Sensors*, vol. 14, pp. 5823-5844, 2014.

[5] T. Yeo, T. Sun, and K. Grattan, "Fibre-optic sensor technologies for humidity and moisture measurement," *Sensors and Actuators A: Physical*, vol. 144, pp. 280-295, 2008.

[6] S. K. Khijwania, K. L. Srinivasan, and J. P. Singh, "An evanescent-wave optical fiber relative humidity sensor with enhanced sensitivity," *Sensors and Actuators B: Chemical*, vol. 104, pp. 217-222, 2005.

[7] Q. Zhou, M. R. Shahriari, D. Kritz, and G. H. Sigel Jr, "Porous fiber-optic sensor for high-sensitivity humidity measurements," *Analytical Chemistry*, vol. 60, pp. 2317-2320, 1988.

[8] J. Mathew, Y. Semenova, G. Rajan, and G. Farrell, "Humidity sensor based on a photonic crystal fiber interferometer," 2010.

[9] H.-N. Li, D.-S. Li, and G.-B. Song, "Recent applications of fiber optic sensors to health monitoring in civil engineering," *Engineering structures*, vol. 26, pp. 1647-1657, 2004.

[10] S. Muto, O. Suzuki, T. Amano, and M. Morisawa, "A plastic optical fibre sensor for real-time humidity monitoring," *Measurement Science and Technology*, vol. 14, p. 746, 2003.

[11] J. M. Corres, I. R. Matias, and F. J. Arregui, "Optical fibre humidity sensors using nano-films," in *Sensors*, ed: Springer, 2008, pp. 153-177.

[12] J. M. Corres, J. Bravo, I. R. Matias, and F. J. Arregui, "Nonadiabatic tapered single-mode fiber coated with humidity sensitive nanofilms," *Photonics Technology Letters, IEEE*, vol. 18, pp. 935-937, 2006.

[13] J. M. Corres, F. J. Arregui, and I. R. Matías, "Sensitivity optimization of tapered optical fiber humidity sensors by means of tuning the thickness of nanostructured sensitive coatings," *Sensors and Actuators B: Chemical*, vol. 122, pp. 442-449, 2007.

[14] G. Brambilla, "Optical fibre nanowires and microwires: a review," *Journal of Optics*, vol. 12, p. 043001, 2010.

[15] A. Stiebeiner, R. Garcia-Fernandez, and A. Rauschenbeutel, "Design and optimization of broadband tapered optical fibers with a nanofiber waist," *Optics express*, vol. 18, pp. 22677-22685, 2010.

[16] T. A. Birks and Y. W. Li, "The shape of fiber tapers," *Lightwave Technology, Journal of*, vol. 10, pp. 432-438, 1992.

[17] J. Lou, L. Tong, and Z. Ye, "Modeling of silica nanowires for optical sensing," *Optics express*, vol. 13, pp. 2135-2140, 2005.
[18] J. Wo, G. Wang, Y. Cui, Q. Sun, R. Liang, P. P. Shum, *et al.*, "Refractive index sensor using microfiber-based Mach–Zehnder interferometer," *Optics letters*, vol. 37, pp. 67-69, 2012.
[19] A. A. Jasim, S. W. Harun, K. S. Lim, B. Rahman, and H. Ahmad, "Microfibre Mach-Zehnder interferometer and its application as a current sensor," *Optoelectronics, IET*, vol. 6, pp. 298-302, 2012.
[20] K. Okamoto, *Fundamentals of optical waveguides*: Academic press, 2010.
[21] G. Y. Chen, M. Ding, T. P. Newson, and G. Brambilla, "A review of microfiber and nanofiber based optical sensors," *The Open Opt. J*, vol. 7, pp. 21-57, 2013.
[22] L. Tong, J. Lou, and E. Mazur, "Single-mode guiding properties of subwavelength-diameter silica and silicon wire waveguides," *Optics Express*, vol. 12, pp. 1025-1035, 2004.